



HAL
open science

Effect of retting on hemp shiv physicochemical properties

Santiago Arufe, Arthur Hellouin de Menibus, Nathalie Leblanc, H el ene Lenormand

► **To cite this version:**

Santiago Arufe, Arthur Hellouin de Menibus, Nathalie Leblanc, H el ene Lenormand. Effect of retting on hemp shiv physicochemical properties. *Industrial Crops and Products*, 2021, 171, pp.113911. 10.1016/j.indcrop.2021.113911 . hal-03383274

HAL Id: hal-03383274

<https://hal.science/hal-03383274>

Submitted on 22 Aug 2023

HAL is a multi-disciplinary open access archive for the deposit and dissemination of scientific research documents, whether they are published or not. The documents may come from teaching and research institutions in France or abroad, or from public or private research centers.

L'archive ouverte pluridisciplinaire **HAL**, est destin ee au d ep ot et  a la diffusion de documents scientifiques de niveau recherche, publi es ou non,  emanant des  tablissements d'enseignement et de recherche fran ais ou  trangers, des laboratoires publics ou priv es.



Distributed under a Creative Commons Attribution - NonCommercial 4.0 International License

1 **Effect of retting on hemp shiv physicochemical properties**

2 **Santiago Arufe^{a*}, Arthur Hellouin de Menibus^{b,c}, Nathalie Leblanc^a, H  l  ne**

3 **Lenormand^a**

4 ^aUniLaSalle, Univ. Artois, ULR 7519 - Transformations & Agro-ressources, Normandie

5 Universit  , F-76130 Mont Saint Aignan, France

6 ^bEco-Pertica, H  tel Buissonnet, 61340 Perche-en-Noc  , France

7 ^cFrench National Association of Short Distribution Network Hemp Producers (Association

8 Nationale des Chanvriers en Circuits Courts), France

9

10 *Corresponding Author: santiago.arufe@gmail.com

11

12 **Abstract**

13 Hemp (*Cannabis sativa L.*) retting is an essential process for the defibrating process to
14 separate hemp shiv and fibres. The goal of this study is to investigate how retting level affects
15 hemp shiv properties that are useful when such particles are used as a building material for
16 insulation applications. Hemp straw samples were taken on the field at 0, 8, 22, 42 and 62
17 days of retting. Shiv and fibres were manually separated in order to obtain hemp shiv to be
18 analysed in the laboratory. Different properties of hemp shiv were measured: colour, density
19 of both hemp shiv (envelope density) and hemp shiv powder (**particle walls** density) and
20 chemical composition (content of ash, lignin, cellulose, hemicellulose and soluble). Colour
21 changes were observed: brightness, greenness and yellowness decreased during retting.
22 During the first 22 days of retting, greenness and yellowness showed the greatest variations,
23 while brightness decreased after 22 days. Envelope density of hemp shiv significantly
24 increased (over 65%) between 22 and 42 days of retting. Nevertheless, **particle walls** density
25 only increased $\approx 6\%$ throughout the whole period of retting. This indicates that the degradation
26 process give access to a part of the closed porosity of unretted hemp shiv. Hemp shiv mass
27 loss during retting achieved $\approx 26\%$ at 62 days of retting. Soluble and hemicellulose were the

28 most affected compounds with a decrease of, respectively, 42 and 45% whereas changes for
29 cellulose and lignin were less pronounced. In conclusion, the retting process changes colour,
30 density and chemical composition of hemp shiv and some possible consequences for building
31 applications were highlighted.

32 **Keywords:** density, porosity, bio-based aggregate, color, sorption, building material

33

34 **1. Introduction**

35 In France, most of the plant particles that are used in construction come from plant stems such
36 as hemp, flax, sunflower, rapeseed, maize, cereals, miscanthus, reed, etc. They might be used
37 alone or mixed with a binder (clay, plaster or lime for instance) to make biobased concrete or
38 wattle and daub. They can be employed in different proportion in order to obtain light or
39 heavy materials, depending on the expected performances (thermal, acoustic insulation,
40 mechanical resistance, etc).

41 Different biobased resources might differ in terms of chemical composition (cellulose,
42 hemicelluloses, pectins and lignins in particular), microstructure and their interactions with
43 water (sorption, absorption). This might affect the biobased concrete making process or *in situ*
44 performance. Differences might also exist within a given type of plant particle, depending on
45 the variety, the soil type and weather conditions or the followed technical itinerary used.

46 A source of variability in hemp production is the retting duration. Retting is an operation
47 commonly used for fibred bio-based resources, like flax or hemp, to ease the subsequent
48 defibration process and to improve the fibres quality (Réquilé et al., 2021). In the past, hemp
49 straw was retted in rivers, but this practice was progressively forbidden to preserve adequate
50 water quality. An alternative practice was to use water ponds for the retting operation,
51 ensuring the water was not brought back to a river. Nowadays, in France, hemp is retted
52 directly on the field. Hemp is cut and then left on the ground several weeks, usually 1 to 4
53 weeks, but it might be up to 10 weeks (Ribeiro et al., 2015). The retting operation is a process
54 involving several microorganisms and activated by the presence of water, due to rain and the

55 day-night cycles and warm conditions. Retting duration is then weather dependant and it
56 cannot be fully controlled by the farmer who has to manage it to achieve a certain retting
57 degree and other needs like, in example, having a relatively dry hemp straw to bale it. As
58 consequence, retting degree depends on the weather (humidity and temperature) and its
59 duration. Consequently, retting is a source of variability on a year per year basis for a farmer,
60 and between farmers situated at different locations.

61 A direct use of agricultural resources for building construction might requires that
62 construction workers accept a given range of variability in the resources. This is not a novel
63 approach since most of French buildings built before 1850 were done with available local
64 resources without the possibility to carry easily alternative materials. However, to guarantee
65 performances with natural resources is a scientific challenge since it needs to identify the
66 variability nature and extent, as well as their impact on the performances of interest when
67 used as a building material. It is also important to identify if there is a maximum variability
68 level acceptable for the material to be used.

69 The constraint on the retting duration differs depending on the application. It might be high
70 for high tech applications, where retting duration should be minimized to optimize hemp
71 fibres mechanical resistance (Placet et al., 2017). Nowadays, the main employed criteria to
72 define retting duration is the obtention of high-quality hemp fibres being hemp shiv usually a
73 by-product of this process. However, retting duration can also impact hemp shiv quality and
74 consequently their different applications. Particularly, hemp shiv applications in green
75 buildings insulation such as: a) as a loose fill raw insulation material without any load to
76 sustain where to prevent creep under its own weight and to ensure a good thermal
77 conductivity is essential, b) for floating floor applications where hemp shiv has to prevent
78 large compression deformation to reach high noise impact reduction for insulation between
79 two floors (Chiasson-Poirier et al., 2021) and c) in bio-based concrete, where shiv can be
80 mixed with clay, gypsum, lime or other mineral binders (Wang et al, 2019; Colinart et al,

81 2020) and soluble compounds that may be lixiviated from hemp shiv to the mixture (mainly
82 pectins, proteins and lipids, Viel et al., 2018).
83 The main aim of this work is to focus on hemp shiv and evaluate the degree of constraint on
84 its retting duration for the aforementioned green building insulation applications analysing the
85 retting impact on properties variability of hemp shiv. This study does not aim to find the
86 optimal duration of retting which would require the study of hemp fibres. For this purpose, the
87 modifications on hemp shiv during the retting process by means of colour, density, water
88 sorption isotherms and water absorption kinetics at 23°C and chemical composition were
89 studied in detail and related to possible consequences for building applications.

90

91 **2. Materials and Methods**

92 **2.1. Hemp Shiv**

93 Hemp (*Cannabis sativa L.*) plants (Fibror variety) were all collected on 19th August 2019 at
94 Le Grand Champrond farm (48.571909, 0.753359, 61290 Moulicent, France). After
95 harvesting they were placed on UniLaSalle garden (3 rue du Tronquet, 76130 Mont St
96 Aignan, France) during a maximum of 62 days for retting. Hemp samples were taken at 0, 8,
97 22, 42 and 62 days of retting and shiv and fibres were manually separated to obtain hemp shiv
98 to be analysed in the laboratory. The whole stem of hemp was employed to obtain hemp shiv
99 after manual defibration. A mean of 15 hemp stems were employed for each batch. Once
100 hemp shiv was obtained, samples of each batch were mixed before measuring in order to
101 homogenize them and obtain a bulk of hemp shiv from different plants and parts of the stem.
102 Only shiv was treated in this study. The fibres obtained from each batch of shiv were however
103 kept for a later study.

104 Ambient conditions (rainfall (www.terre-net.fr), relative humidity and ambient temperature)
105 were recorded (Figure 1). Such an uncontrolled approach ensures the retting process is fully
106 representative of field conditions in terms of weather and microorganisms' activity among
107 others.

108

109 **2.2. Colour**

110 Colour determination of hemp shiv powders was carried out using a spectrophotometer (CM-
111 2300d, Konika Minolta, Japan). Colour was measured by means of CIELab coordinates (ISO
112 11664-4:2008): L* (whiteness ($L^*=0$) or brightness ($L^*=100$)), a* (redness ($a^*>0$) or
113 greenness ($a^*<0$) and b* (yellowness ($b^*>0$) or blueness ($b^*<0$)). Hemp shiv powders were
114 obtained after milling of hemp shiv (previously drying until constant weight at 40°C)
115 employing a micro impact mill (Culatti, Switzerland). The rotor speed was adjusted to 7
116 (≈ 3000 rpm) and a standard sieve of 1 mm of mesh size was employed.
117 Colour determination was carried out on milled samples due to irregular surface of hemp shiv
118 led to shadows which prevented the obtaining of repeatable measurements. Colour
119 determination on powdered samples allowed measurements with better quality allowing a
120 comparison of colour between samples.

121

122 **2.3. Chemical Composition**

123 The chemical composition of samples (content of ash, lignin, cellulose, hemicellulose and
124 soluble) was determined following the Van Soest method (AFNOR, 1997, Viel et al., 2018)
125 employing an adapted machine (FibertcTR 8000, Foss, Denmark). To carry out this
126 measurement all samples were previously dried until constant weight at 40°C and then milled
127 employing a micro impact mill (Culatti, Switzerland), the rotor speed was adjusted to 7 and a
128 standard sieve of 1 mm of mesh size was employed.
129 Mass loss during retting was determined throughout the mean value obtained after weighing
130 several particles (60) with similar size (length: 7.6 ± 1.3 mm and width: 2.01 ± 0.4 mm) of each
131 batch of samples, considering that the first batch (0 days of retting) had no mass loss. For
132 those samples showing a mass loss during retting, the chemical composition was pondered
133 taking into account this process (mass loss, solubles, hemicellulose, lignin, ash represent
134 100 % of the hemp shiv mass). All measurements were carried out at least in triplicate.

135

136 **2.4. Density**

137 Density of both hemp shiv (envelope density) and hemp shiv powder (**particle walls** density)
138 was calculated after measurement of sample volume by gas displacement using a gas
139 pycnometer (Pycnomatic Evo, ThermoScientific) with argon as employed gas. Gas was
140 introduced into a small vessel (21.42 cm³) at a constant temperature of 23°C. The pressure (P)
141 was set at 1 bar (with highest and lowest limit of 1.5 bar and 0.5 bar, respectively) considering
142 that sample is in equilibrium when ΔP between different measurements is lower than 0.00020
143 bar and volume standard deviation lower than 0.050%. Envelope density was then calculated
144 by ratio of sample mass and sample volume determined by gas displacement (Glé et al.,
145 2021). Each sample was measured at least in duplicate.

146 Once both **particle walls** and envelope density were obtained, closed porosity was calculated
147 as follows (Glé et al., 2021), Eq. (1):

148

$$149 \theta_{closed} = 1 - \frac{\rho_{envelope}}{\rho_{pwall}} \quad (1)$$

150

151 where θ_{closed} corresponded to closed porosity (-), $\rho_{envelope}$ and ρ_{pwall} to envelope and **particle**
152 **walls** density (kg/m³) of samples determined as previously explained, respectively.

153

154 **2.5. Scanning electron microscopy (SEM)**

155 Image of samples were taken employing scanning electron microscopy (JSM-IT100 LA,
156 JEOL, Japan) under vacuum conditions (40 Pa) and an accelerating voltage of 15 kV.

157

158 **2.6. Water sorption isotherms**

159 Water sorption isotherms of samples were determined at 23°C using a Dynamic Vapour
160 Sorption machine (DVS, SPS-Sorption Test System, proUmid), employing nitrogen as gas in

161 order to control relative humidity. At least duplicate samples (219 ± 34 mg as average sample
162 weight) were measured. Different equilibrium points were determined corresponding to a
163 fixed relative humidity (ϕ): 0, 0.05, 0.10, 0.15, 0.20, 0.30, 0.35, 0.50, 0.75, 0.85 and 0.90 for
164 adsorption experiments and 0, 0.15, 0.30, 0.35, 0.50, 0.75, 0.85, 0.90 for desorption
165 experiments. Samples employed for adsorption experiments were previously dried until a
166 constant weight was obtained in an oven at 40°C . Desorption samples were previously
167 exposed to a relative humidity of 90% at 23°C , using the DVS, for hydration until they
168 reached a constant weight.

169 Guggenheim-Anderson-de Boer (GAB, van den Berg and Bruin (1981)) and BET models
170 (Brunauer *et al.*, 1938) were employed to fit water sorption experimental data (equilibrium
171 moisture content, X_{eq} , and relative humidity, ϕ) by Eq. (2) and Eq. (3) respectively:

172

$$173 \quad X_{eq} = \frac{X_m K C \phi}{(1 - K \phi)(1 - K \phi + C K \phi)} \quad (2)$$

174

$$175 \quad X_{eq} = \frac{X_m C \phi}{(1 - \phi)(1 + (C - 1)\phi)} \quad (3)$$

176

177 where X_m is the monolayer moisture content (kg water/kg dried solid, d.b.), C (dimensionless,
178 -) and K (dimensionless, -) is a parameter related to the heat of sorption of the multilayer in
179 GAB model. BET was applied in the range of relative humidity from 0.05 to 0.35 in order to
180 determine the specific surface area (Collet *et al.*, 2008) of samples assuming that X_m of BET
181 model represents the quantity of water molecules that covers the entire surface as a monolayer
182 and no diffusion of water through the material taken place. Experimental data was modelled
183 using these two methods employing Solver function of Excel software. In the case of BET
184 model, once model parameters were obtained, specific surface area was calculated as follows,
185 Eq. (4):

186

187
$$a_s = \frac{X_m L a_m}{M_w} \quad (4)$$

188

189 where a_s is the specific surface area of the sample (m^2/g), L the Avogadro constant ($6.023 \cdot 10^{23}$
190 mol^{-1}), a_m cross sectional area of water molecule ($1.08 \cdot 10^{-19} \text{ m}^2$) and M_w molecular weight
191 of water molecule ($18 \text{ g} \cdot \text{mol}^{-1}$).

192

193 **2.7. Water absorption kinetics**

194 Water absorption kinetics of different samples were determined at 5, 15, 60, 480, 1440, 2880
195 min employing a protocol based on the one previously published by Amziane and Collet
196 (2017) but with some modifications. Samples ($M_0 \approx 1 \text{ g}$) previously dried at 40°C until
197 constant weight were put in water bath (water temperature $23.0 \pm 0.5^\circ\text{C}$) during different
198 periods of time employing a tea strainer ball. Liquid/Solid ratio was higher than 300 assuring
199 conditions of infinite dilution. Once the desired time of immersion was achieved, samples
200 were removed and filtered by vacuum filtration with a büchner funnel using a paper filter, in
201 order to eliminate the excess of water on the surface of the material, and finally weighed to
202 determine the mass of the sample after immersion (M_t , g). Afterwards, samples were dried in
203 an oven at 105°C until constant weight ($M_{105^\circ\text{C}}$). Each point of water absorption kinetics was
204 carried out at least in triplicate.

205 Different parameters to study water absorption kinetics were calculated: water absorption
206 related to initial dry mass (WA_{M_0} , kg water/kg initial dry mass, Eq. (5)); water absorption
207 related to final dry mass (WA_{M_F} , kg water/kg final dry mass, Eq. (6)) and solid loss during
208 immersion (SL , kg lost dry solid/kg final dry mass, Eq. (7)):

209

210
$$WA = \frac{M_t}{M_0} \quad (5)$$

211

212
$$WA = \frac{M_t}{M_{105^\circ\text{C}}} \quad (6)$$

213

$$214 \quad SL = \frac{M_0 - M_{105^\circ C}}{M_{105^\circ C}} \quad (7)$$

215

216 These parameters were finally modelled employing a function developed by Nagy and Vas
217 (Nagy and Vas, 2003) that gives an asymptotically correct approximation of the capillary
218 water uptake process for both $t \rightarrow 0$ and $t \rightarrow \infty$, Eq. (8):

219

$$220 \quad \Delta m(t) = \Delta m_\infty (1 - e^{-At^{\frac{1}{2}B}})^B \quad (8)$$

221

222 where A and B are constant parameters, Δm_∞ is the modelled parameter related to equilibrium
223 (when $t \rightarrow \infty$) and $\Delta m(t)$ is the experimental data of water absorption kinetics (W_{AM0} , W_{AMF}
224 or SL).

225

226 **2.8. Statistical analysis**

227 Experimental data were statistically analysed as mean \pm standard deviation. The goodness of
228 the adjustment of each model was determined based on the method of least squares.

229

230 **3. Results and Discussion**

231 Figure 1 shows the temperature-moisture cycles and the rainfall during retting. Hemp
232 experienced cycles of temperature between 5 to 45°C and ranges of relative humidity between
233 20% to 100 %. Even if the experiment was carried out in late summer, samples experienced at
234 least 2h per day at 100% of relative humidity every day, due to dew during the night. Samples
235 retted more than 42 days experienced cycles with higher relative humidity due to
236 precipitations that occurred during that time of the experiment (month of October).

237

238 *Location of Figure 1*

240 **3.1. Colour**

241 Photographs of samples at each retting duration are presented in Figure 1. Colour evolves
242 clearly with the retting duration throughout the 62 days. Initially with a yellow-green
243 predominance at “naked eye”, the colour darkens as the retting progresses, until it becomes
244 almost black. Regarding colour parameter values (Table 1) samples lost brightness, (decrease
245 of L* parameter from 85 to 65), greenness (slightly increase of a* parameter from -0.62 to
246 1.22) and yellowness (decrease of b* parameter 19.78 to 9.57) with retting time. Bleuze et al.
247 (2020) reported a similar behaviour for colour parameters of hemp stem subjected to
248 simulated rains and dews to carry out retting under laboratory conditions for 42 days at 15°C.
249 Mazian et al. (2018) described a similar trend of colour after a visual analysis of hemp fibres
250 (loss of brightness and appearance of darken (grey) spots) and reported hemp stems to have a
251 similar colour. Colour variations could be related to different chemical modifications on
252 samples (such as the moisture of the sample) and/or colonization of fungi (Akin et al., 2000,
253 Martin et al., 2013, Bleuze et al., 2020). Loss of brightness and the darken trend are attributed
254 to the development of microbial communities (fungal and bacteria, Ribeiro et al., 2015).
255 Moreover, according to Mazian et al. (2018) the microbial communities would start to
256 colonize the stems surface after 3 weeks of retting and gradually cover the entire stems at the
257 end of retting. This behaviour is observed on the studied samples, where a significant
258 decrease on brightness (L* parameter) takes place when retting was longer than 22 days
259 (Table 1).

260

261 **3.2. Chemical composition**

262 The chemical composition of samples is shown in Table 1 and Figure 2. Mass loss during
263 retting achieved a maximum of 26% of initial mass at 62 days of retting. During the period
264 between 8 and 22 days, the highest mass loss was observed ($\approx 15\%$). This is in the same order
265 of magnitude of Delannoy et al. (2018) that reported a mass loss of $\approx 15\%$ after 3 months

266 using an ageing protocol at a constant temperature of 30°C and humidification and drying
267 cycles with 5 days at 98% of relative humidity and 2 days at 40% of relative humidity. Ashes,
268 hemicellulose and soluble compounds were the components more affected by retting being
269 reduced by $\approx 54\%$, $\approx 44\%$ and $\approx 42\%$, respectively. On the other hand, cellulose ($\approx 15\%$) and
270 lignin (invariable) were less affected. This could be due to the fact that pectins (main
271 component of soluble compounds) and partially hemicellulose are more soluble in water than
272 cellulose (Gao et al., 2014; Silva et al., 2014). Soluble compounds significantly decreased
273 during the first 22 days of retting (from 21.1 to 12.9 g/100 g dry solid). Reduction of
274 hemicellulose and ashes was steady during this period. This fact seems to indicate that, at
275 least on the first days of retting, the main compounds that are eliminated from the hemp shiv
276 are those measured as soluble compounds. As consequence mass loss kinetics during retting
277 could be separated during two main phases. A first phase, mainly characterized by the loss on
278 soluble compounds and hemicellulose and a second one which is mainly related to the
279 degradation of the other compounds while soluble compounds remain constant.

280 Chemical composition of studied samples of hemp shiv were in the range of those previously
281 published in literature (Amziane and Collet (2017), Chabriac et al., 2016, Diquélou et al.,
282 2015, Viel et al., 2018) except in the case of soluble compounds where values were higher for
283 the two first samples (0 and 8 days of retting). They varied between 21.1 and 12.3 g/100 g dry
284 solid which is a higher that the range observed in literature 17-5%. Reported values of hemp
285 shiv soluble compounds on literature usually correspond to retted hemp but often no
286 information about retting duration and conditions are provided. In this sense, literature values
287 may be lower than those reported in this study due to soluble compounds lixiviation during
288 the first days of retting. In **this** case, the studied samples had different retting durations and
289 mass loss during retting and this has been taken into account in order to calculate the soluble
290 compounds percentage.

291

292 *Location of Figure 2*

293

294 **3.3. Density**

295 Envelope density of hemp shiv significantly increased (over 65%) between 22 and 42 days of
296 retting. No significant difference was observed for a retting duration longer than 42 days in
297 Table 1. **Particle walls** density of hemp shiv (powdered samples) increased slightly compared
298 to envelope density, a $\approx 6\%$ increase was observed throughout the whole period of retting
299 (from 1463 up to 1553 $\text{kg}\cdot\text{m}^{-3}$). These values are similar to those previously reported for the
300 density of cell wall for hemp shiv (1450 $\text{kg}\cdot\text{m}^{-3}$ (Picandet, 2017)) or flax and hemp fibres
301 (1480-1500 $\text{kg}\cdot\text{m}^{-3}$ (Garcia-Jaldon et al., 1998)). These trends of envelope and **particle walls**
302 density indicate an evolution of porosities due to the degradation process by microorganisms
303 that takes place during retting. Hemp shiv is a porous material having external and internal
304 pores (Chabriac et al., 2016). Some internal pores are not accessible when measuring using
305 the employed technique because they are located inside the material (closed porosity).
306 However, due to retting these pores became accessible by degradation of the material and, as
307 consequence, they became measurable by the employed technique. Consequently, increasing
308 retting time allowed the measurement of these pores and hence lead to the determination of a
309 lower volume for a similar amount of mass. This behaviour can be clearly observed regarding
310 closed porosity (Eq. (1)) parameter, Table 1, which decreases by a half, from ≈ 0.50 to ≈ 0.25
311 between 22 and 42 days of retting with no differences before and after this period of time.
312 This observed result suggests that the main variations in terms of sample porosity take place
313 in this period which, even if the studied retting in the present study is particular (a specific
314 field, a specific weather, etc), it is in agreement with common period of harvesting employed
315 by farmers (Martin et al., 2013). Moreover, relating this behaviour with previous colour trends
316 (mainly a^* and b^* parameters) both match on the fact that after 42 days and up to 62 days of
317 retting no-significant differences are observed.

318

319 **3.4. Scanning electron microscopy (SEM)**

320 Figure 3 shows SEM images of samples obtained after 22 and 42 days of retting. Hemp shiv
321 come from xylem and phloem, some vascular tissues providing transports of proteins, sugars,
322 minerals. They are composed by cells that are composed by layers of primary wall (thickness
323 10 nm), second wall and plasma membrane (thickness 250 nm). Cells are linked between
324 them by middle lamella (thickness 10 nm) (Viel et al., 2018). Pectins (one of the main
325 compounds measured as soluble compounds) are mainly present in middle lamella whereas
326 hemicellulose, cellulose and lignin are mainly located in primary and second walls. Changes
327 of chemical compositions observed between 0 and 22 days (reduction of soluble and
328 hemicellulose) did not cause significant structural modification due to low thickness of tissues
329 (middle lamella and primary wall) composed by these macromolecules. On the other hand,
330 once middle lamella and primary wall were degraded during the first 22 days of retting,
331 structural modification has become visible by a degradation of second wall, thicker than
332 middle lamella and primary wall, and involved an increase of density and reduction of closed
333 porosity. Figure 3 illustrates structural modification by showing looseness of walls between
334 samples of 22 days and 42 days of retting. **No clear modifications were observed between S42
335 and S62.** This trend has been confirmed by values of closed porosity, Table 1.

336

337 *Location of Figure 3*

338

339 **3.5. Water sorption isotherms**

340 Experimental data of water sorption isotherms at 23°C showed different behaviours as
341 function of retting time, Figure 4 (a and b). A decrease on equilibrium moisture content at
342 high relative humidity values (>0.90), from 0.55 to 0.22 kg H₂O/kg dry solid, was observed
343 between 0 and 22 days of retting, with no great differences between samples retted more than
344 22 days. On the other hand, at intermediates relative humidity values (0.35-0.70) an increase
345 on equilibrium moisture content was observed for samples retted more than 22 days compared
346 to those less retted. Similar behaviour was previously reported for aging hemp shiv (Delannoy

347 et al., 2018) between 0.20 and 0.80 of relative humidity. This behaviour could be related to
348 structural changes on samples leading to new structures that are able to retain more water
349 molecules. As it was aforementioned, the degradation process during retting may cause a pore
350 opening leading to a decrease of closed porosity for the most retted samples. These pores,
351 previously not accessible, became available for water molecules to be adsorbed and hence
352 increasing the equilibrium moisture content of the sample. However, this phenomenon was
353 not observed in the case of high relative humidity values (>0.75) where more retted samples
354 showed lower values of equilibrium moisture content. This result could be explained by the
355 relative amount of hydrophilic compounds (solubles, hemicellulose and cellulose) on each
356 sample and their location. Even if the sum of these hydrophilic compounds always represents
357 $\approx 88\%$ of sample mass (without considering mass loss), the proportion between the 3 types of
358 compounds is different depending on retting duration. As retting duration increases, the ratio
359 of each hydrophilic compound over the total amount of hydrophilic compounds (g of X
360 compound/100 g total hydrophilic compounds) changes differently. In fact, it was observed
361 that solubles and hemicellulose ratios decrease both from 24 to 19 g/100 g hydrophilic
362 compounds whilst cellulose ratio increases. Tissues are complex matter where
363 macromolecules are tangled. When some pectins (soluble compounds) and hemicellulose are
364 degraded at the beginning of the retting process, the access of cellulose and lignin molecules
365 are improved but limited by the rest of pectin and hemicellulose surrounding them. So the
366 more the sample is retted, the less the quantity of hydrophilic compounds at the vascular
367 surface. Consequently, the capacity of these samples to retain water at higher relative
368 humidity is also reduced.

369 Experimental water sorption isotherms at 23°C were satisfactorily modelled employing GAB
370 and BET models ($R^2 > 0.997$), Table 2. GAB model parameters satisfactorily corroborate the
371 trends observed on experimental data related to the increase of equilibrium moisture content
372 with retting time (≤ 22 days) at intermediates relative humidity values and its decrease at
373 higher values (< 0.75). In the case of BET model, the use of this model allowed the

374 determination of a specific surface area of samples, a_s , Table 2. Specific surface area
375 significantly increased from 8 to 22 days and from 22 to 42 days of retting. The significant
376 increase of this parameter could be also related to the pore opening process during retting
377 previously mentioned which makes a higher surface available for water to be adsorbed. In this
378 case, the trend did not exactly correspond to the one observed for **particle walls** density.
379 **Particle walls** density significantly increased only when retting more than 22 days whereas
380 employing this technique an intermediate increase was already observed between 8 and 22
381 days. This difference may be related to the sensitivity of the methods used suggesting that
382 dynamic water sorption analysis could be more sensitive than densities measurements when
383 determining changes on the internal structures of hemp shiv on the range of application of
384 BET model (0.05-0.35 of relative humidity).
385 Summarising, effect of retting on water sorption behaviour of hemp shiv could be explained
386 by the combined effect of chemical modification and degradation of microstructure. Chemical
387 modification seems to be responsible of the different equilibrium moisture contents at high
388 relative humidity values (>0.80) whereas porosity changes on hemp shiv may be related to the
389 equilibrium moisture contents at intermediates relative humidity values.

390

391 *Location of Figure 4a and 4b*

392

393 **3.6. Water absorption kinetics**

394 Figure 5a shows the water absorption kinetic of hemp shiv retted 22 days as example. In the
395 case of water uptake, water gain of samples was at least already 50% (dry basis) on the first
396 15 min of immersion indicating that water absorption mainly occurs at the beginning of the
397 immersion. Solid loss during immersion (SL) takes place also at the first minutes of
398 immersion and after 15 min it is asymptotic up to 48 h. Note here that other authors (Glé and
399 Gourlay 2015) previously reported that hemp shiv immersed in water could lose solid matter
400 during at least 100 days. No great difference between water absorption kinetics of different

401 retted samples is observed (Figure 5b) but unretted sample water absorption was always
402 higher, probably due to the chemical composition of samples. As it was previously mentioned
403 in the case of water sorption, retted samples may have lower amounts of hydrophilic
404 compounds due to their loss during retting. The fact that retted samples did not present
405 different WA kinetics may suggest that chemical composition is not the single parameter to
406 manage water absorption kinetics and this process may be influenced by other parameters
407 such as the microstructure of the sample. The values of WA of retted samples were similar of
408 those observed in other studies (Delannoy et al., 2018).

409 Nagy and Vas model satisfactorily fitted experimental data ($R^2 > 0.970$). In the case of WA,
410 experimental values at 48 h were very similar to those obtained for Nagy and Vas model
411 parameter related to equilibrium (WA_{∞}), Table 3, which indicates that 48 h can be a
412 reasonable amount of time for hemp shiv to be considered closed to equilibrium during
413 immersion. Regarding SL, Nagy and Vas model parameter related to equilibrium (SL_{∞})
414 showed a 20 to 11% decrease on solid loss with retting. This decrease is in accordance with
415 the trend obtained by Van Soest method for soluble compounds content, which was also lower
416 for those samples retted during a large period. This fact suggests that solid loss may be related
417 mainly to soluble compounds that are eliminated from the samples during immersion, at least
418 at the beginning of the retting. Moreover, the accordance between values of SL_{∞} (Table 3) and
419 soluble compounds may suggest that water immersion of samples during 48 h and a
420 subsequent drying of samples until constant weight in order to determine solid loss could be a
421 good method to have a rough estimation of the quantity of water-soluble compounds of hemp
422 shiv samples. Even if during Van Soest method different solvents and temperatures are
423 employed to eliminate soluble compounds from the sample.

424

425 *Location of Figure 5a and 5b*

426

427 **3.7. Variability consequence for construction workers**

428 Retting has direct implications on hemp shiv properties. The porous structure is modified
429 together with the chemical composition and the hygroscopic behaviour at high relative
430 humidity values. In addition, a blind manual manipulation by a construction worker used to
431 hemp shiv showed retted hemp shiv seems stiffer and less flexible than unretted shiv. This is
432 in agreement with (Chiasson-Poirier et al., 2021) who found that retted shiv is more resistant
433 to compression at high stress level (higher than 200 kPa) than unretted hemp shiv. The shiv,
434 even the most retted one studied here, does not disaggregate when manipulated. If this would
435 be the case, the shiv would clearly be inappropriate for building applications.

436 Taking into account the modifications induced by retting, the question for a green building
437 professional is to define the acceptable range of retting depending on the application. First, for
438 a loose fill raw insulation material without any load to sustain, for instance to insulate ceilings
439 within a wood frame, two parameters are essential: to prevent creep under its own weight and
440 to ensure a good thermal conductivity. Material creep under its own weight was not studied to
441 our knowledge, however, since retting makes the shiv stiffer, it is likely that retting would not
442 induce a worse performance than unretted shiv. Regarding the thermal conductivity, it might
443 vary since retting affects the porous structure. A model proposed by (Nguyen et al., 2016)
444 indicates that increasing porosity level would decrease the thermal conductivity since the
445 solid matter is more conductive than air. Retting might induce a slightly higher total porous
446 level, but the main effect at the retting level studied is to convert part of closed porosity to
447 open one **after more than 22 days in this specific study**. The precise effect of retting on the
448 thermal conductivity can be focused in further studies.

449 Second, for floating floor applications where hemp shiv is compressed, the essential
450 parameter is to ensure hemp shiv maintains sufficient stiffness to prevent from large
451 compression deformation. The study (Chiasson-Poirier et al., 2021) showed no essential
452 difference on a unretted and a more retted batch of particles at load level representative of
453 floating floor application, even if retted shiv is stiffer at higher loads (higher than 200 kPa) as
454 stated above. **Regarding noise impact reduction, Lenormand et al., (2017) stated that when**

455 intraparticle porosity is constituted by almost closed pores (first days of retting in this study),
456 acoustical propagation and dissipation become more difficult to occur. However, interparticle
457 pores are more permeable to sound wave and provide greater sound absorption. Hence, it
458 could be expected that retting may have a positive influence on sound absorption of hemp
459 shiv because when retting process takes place led to a decrease on closed porosity (more than
460 22 days in this specific study).

461 Finally, in bio-based concrete, shiv can be mixed with clay, gypsum, lime or other mineral
462 binders. There is no clear change induced by retting on the water absorption kinetic (unless
463 for completely unretted shiv). Thus, the shiv behaviour in the mixer, with water and binder,
464 might not depend much on the retting level. Recent studies have shown that soluble
465 components from plant aggregates could negatively affect the setting time and carbonation of
466 lime-based binders or cement (Delannoy et al., 2020, Diquélou et al., 2015, Wang et al.,
467 2019). On the other hand, the soluble components might have an interesting impact when clay
468 binder is used, since using water in which bio-based resources were fermented is a common
469 practice by unfired clay professional workers to improve clay plaster resistance. Another
470 interesting result is the reduction of the hygroscopic range for retted shiv, which reduces the
471 amount of water in hemp shiv at high relative humidity level. Since water quantity is a key
472 parameter that drives the degradation kinetic of bio-based resources, using retted shiv might
473 even result in a higher durability than using unretted shiv.

474

475 **4. Conclusions**

476 Retting process induces changes in the physicochemical properties of hemp shiv. It reduces
477 brightness, greenness and yellowness colour predominance, closed porosity and mainly the
478 quantity of soluble compounds, hemicellulose and ash. Retting duration decreased the
479 equilibrium moisture content of hemp shiv at high relative humidity atmospheres while on the
480 water absorption kinetics only unretted had a different behaviour of all studied samples, with
481 no differences between retted samples. Consequently, regarding hemp shiv potential

482 applications on green building, the retting level does not significantly affect the applications
483 for loose fill raw insulation and floating floor application. For bio-based concrete with lime or
484 cement, it seems that retted shiv would be preferable to improve the setting or at least not
485 negatively affect it. When clay binder is used, the retting level is not an issue. Indeed, the
486 material reinforcement due to soluble compounds, if any, is not crucial since hemp-clay is
487 considered as a non-bearing material. Eventually, using retted hemp in bio-based concrete
488 might even improve material durability due to the reduction of the hygroscopicity at high
489 humidity level. The 2 months real retting process used in this study was not sufficient to make
490 hemp shiv inappropriate for use in construction.

491

492 **CRedit authorship contribution statement**

493 Santiago Arufe: Conceptualization; Investigation; Validation; Writing original draft, review
494 and editing.

495 Arthur Hellouin de Ménibus: Conceptualization; Investigation; Validation; Writing review
496 and editing.

497 Nathalie Leblanc: Investigation; Validation; Writing review and editing.

498 H el ene Lenormand: Conceptualization; Investigation; Validation; Writing review and editing.

499

500 **Declaration of Competing Interest**

501 The authors report no declarations of interest.

502

503 **Acknowledgements**

504 The authors acknowledge the financial support of the Normandie region and ERDF for the
505 research project TIGRE, the Parc Naturel R egional du Perche and Phillippe Lambert for
506 kindly providing the samples.

507

508 **References**

509 AFNOR, 1997. NF V 18-122-Aliments des animaux-Détermination séquentielle des
510 constituants pariétaux-Méthode par traitement aux détergents neutre et acide et à
511 l'acide sulfurique.

512 Akin, D. E., Epps, H. H., Archibald, D. D., Shekhar, H. S. (2000). Color Measurement of Flax
513 Retted by Various Means. *Text. Res. J.* 70. 852-858.

514 Amziane, S., Collet, F., 2017. *Bio-aggregates Based Building Materials*, Vol. 23 of RILEM
515 State-of-the-Art Reports, Springer Netherlands, Dordrecht.

516 Brunauer, S., Emmet, P.H., Teller E., 1938. Adsorption of gases in multimolecular layers. *J.*
517 *Am. Chem. Soc.* 60, 309-19.

518 Bleuze, L., Chabbert, B., Lashermes, G., Recous, S., 2020. Hemp harvest time impacts on the
519 dynamics of microbial colonization and hemp stems degradation during dew retting.
520 *Ind. Crop. Prod.* 145, 112122.

521 Chabriac, P.A., Gourdon, E., Glé, P., Fabbri, A., Lenormand, H., 2016. Agricultural by-
522 products for building insulation: Acoustical characterization and modelling to predict
523 micro-structural parameters. *Const. Buil. Mater.* 112, 158–167.

524 Chiasson-Poirier, L., Lecompte, T., Hellouin de Menibus, A., 2021. Static and long term
525 compression behavior of hemp shiv for floating floor application. *Const. Buil. Mater.*
526 268 121220.

527 Colinart, T., Vincelas, T., Lenormand, H., Hellouin de Ménibus, A., Hamard, E., Lecompte,
528 T., 2020. Hygrothermal properties of light-earth building materials. *J. Build. Eng.*
529 29:101134.

530 Collet, F., Bart, M., Serres, L., Miriel, J., 2008. Porous structure and water vapour sorption of
531 hemp-based materials. *Const. Buil. Mater.* 22, 1271-1280.

532 Delannoy, G., Marceau, S., Glé, P., Gourlay, E., Guéguen-Minerbe, M., Diafi, D., Nour, I.,
533 Amziane, S., Farcas, F., 2018. Aging of hemp shiv used for concrete. *Mater. Des.* 160,
534 752–762.

535 Delannoy, G., Marceau, S., Glé, P., Gourla. E, Guéguen-Minerbe, M., Diafi, D., Amziane, S.,
536 Farcas, F., 2020. Impact of hemp shiv extractives on hydration of Portland cement.
537 Const. Buil. Mater. 244, 118300.

538 Diquélou, Y., Gourlay, E., Arnaud, L., Kurek, B., 2015. Impact of hemp shiv on cement
539 setting and hardening: Influence of the extracted components from the aggregates and
540 study of the interfaces with the inorganic matrix. Cem. Concr. Compos. 55, 112–121.

541 Garcia-Jaldon, C., Dupeyre, D., Vignon, M., 1998. Fibres from semi-retted bundles by steam
542 explosion treatment. Biomass Bioenergy 14, 251-260.

543 Gao, X., Kumar, R., Wyman, C.E., 2014. Fast hemicellulose quantification via a simple one-
544 step acid hydrolysis. Biotechnol. Bioeng. 111, 1088–1096.

545 Glé P., Gourlay E., 2015. Rapport de recherche MABIONAT, Étude de l'influence de la
546 teneur en eau et du vieillissement sur les performances acoustiques et thermiques des
547 matériaux biosourcés.

548 Glé, P., Lecompte, T., Hellouin de Ménibus, A., Lenormand, H., Arufe, S., Château, C.,
549 Fierro, V., Celzard, A. (2021). Densities of hemp shiv for building: From multiscale
550 characterisation to application. Ind. Crop. Prod. 164, 113390.

551 ISO 11664-4:2008, 2008. Colorimetry - Part 4: CIE 1976 L*a*b* Colour space.

552 **Lenormand, H., Glé, P., Leblanc, N., 2017. Investigation of the acoustical and thermal**
553 **properties of sunflower particleboards. Acta Acust united Ac. 103, 149–157.**

554 Martin, N., Mouret, N., Davies, P., Baley, C., 2013. Influence of the degree of retting of flax
555 fibers on the tensile properties of single fibers and short fiber/polypropylene
556 composites. Ind. Crop. Prod. 49, 755-767.

557 Mazian, B., Bergeret, A., Bénézet, J. C., Malhautier, L. (2018). Influence of field retting
558 duration on the biochemical, microstructural, thermal and mechanical properties of
559 hemp fibres harvested at the beginning of flowering. Ind. Crops Prod. 116, 170-181.

560 Nagy, V., Vas, L. M., 2003. Inrayarn Porosity and Pore Size in Polyester Staple Yarns. In:
561 International Textile Design and Engineering Conference Proceedings, Eninburgh,
562 United Kingdom, pp. 201-208.

563 Nguyen, S.T., Tran-Le, A.D., Vu, M.N., To, Q.D., Douzane, O., Langlet, T., 2016. Modeling
564 thermal conductivity of hemp insulation material: A multi-scale homogenization
565 approach. *Build. Environ.* 107, 127-134.

566 Picandet, V., 2017. Bulk density and compressibility, in: A. S. A. C. F (Ed.), *Bio-aggregates*
567 *Based Building Materials*, RILEM State-of-the-Art reports, 23, Springer, Dordrecht,
568 pp. 167–187.

569 Placet, V., Day, A., Beugrand, J., 2017. The influence of unintended field retting on the
570 physicochemical and mechanical properties of industrial hemp bast fibres. *J. Mater.*
571 *Sci.* 52, 5759-5777.

572 Réquillé, S., Mazian, B., Grégoire, M., Musio, S., Gautreau, M., Nuez, L., Day, A., Thiébeau,
573 P., Philippe, F., Chabbert, B., Chamussy, A., Shah, D.U., Beaugrand, J., Placet, V.,
574 Benezet, J.C., le Duigou, A., Bar, M., Malhautier, L., De Luycker, E., Amaducci, S.,
575 Baley, C., Bergeret, A., Bourmaud, A., Ouagne, P., 2021. Exploring the dew retting
576 feasibility of hemp in very contrasting European environments: Influence on the tensile
577 mechanical properties of fibres and composites. *Ind. Crop. Prod.* 164, 113337.

578 Ribeiro, A., Pochart, P., Day, A., Mennuni, S., Bono, P., Baret, J.L., Spadoni, J.L., Mangin, I.,
579 2015. Microbial diversity observed during hemp retting. *Appl. Microbiol. Biotechnol.*
580 99, 4471-4484.

581 Silva, A.S., Nunes, C., Coimbra, M.A., Guido, L.F., 2014. Composition of pectic
582 polysaccharides in a Portuguese apple (*Malus domestica Borkh.* cv Bravo de Esmolfe).
583 *Sci. Agric.* 71, 331–336.

584 Van Den Berg, C., Bruin, S., 1981. Water activity and its estimation in food systems:
585 theoretical aspects. In L. B. Rockland and G. F. Stewart (Eds.), pp. 1-61.

586 Viel, M., Collet, F., Lanos, C., 2018. Chemical and multi-physical characterization of agro-
587 resources' by-product as a possible raw building material. *Ind. Crop. Prod.* 120, 214-
588 237.

589 Wang, L., Lenormand, H., Zmamou, H., Leblanc, N., 2019. Effect of Soluble Components
590 From Plant Aggregates on the Setting of the Lime Based Binder. *J. Renew. Mater.* 7,
591 903-913.

592

593 **Caption for Figures**

594 **Figure 1.** Evolution of ambient conditions (temperature (red line, -) and relative humidity
595 (blue line, -) during 62 of retting and images of obtained hemp shiv.

596 **Figure 2.** Chemical composition of hemp shiv retted during different time periods.

597 **Figure 3.** SEM images of hemp shiv samples after 22 (A) and 42 (B) days of retting.

598 **Figure 4a.** Water adsorption isotherms of hemp shiv retted during different time periods.

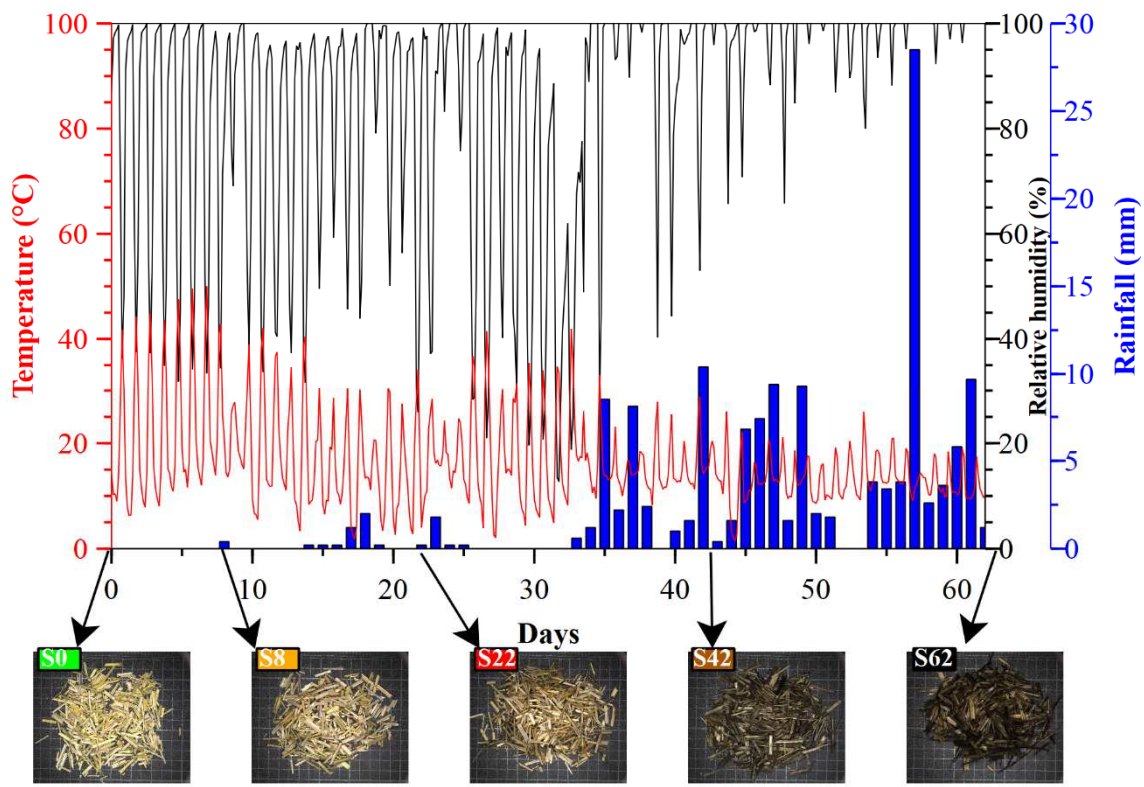
599 Lines correspond to GAB model, Eq. (2).

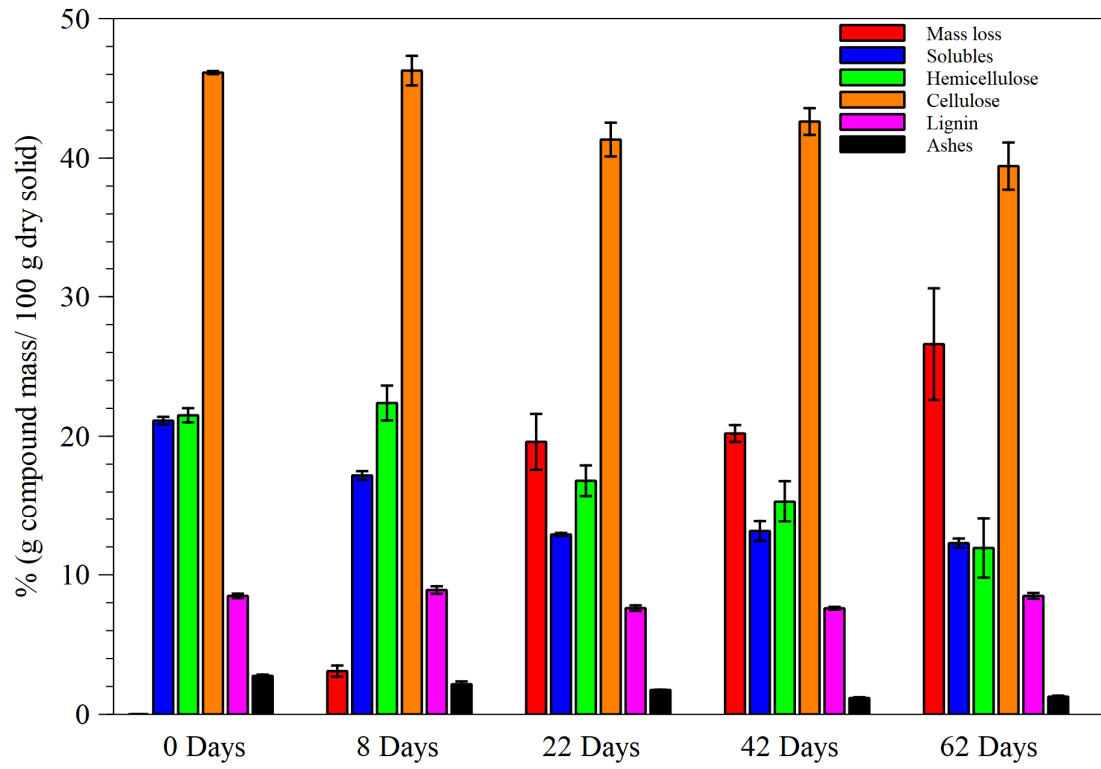
600 **Figure 4b.** Water desorption isotherms of hemp shiv retted during different time periods.

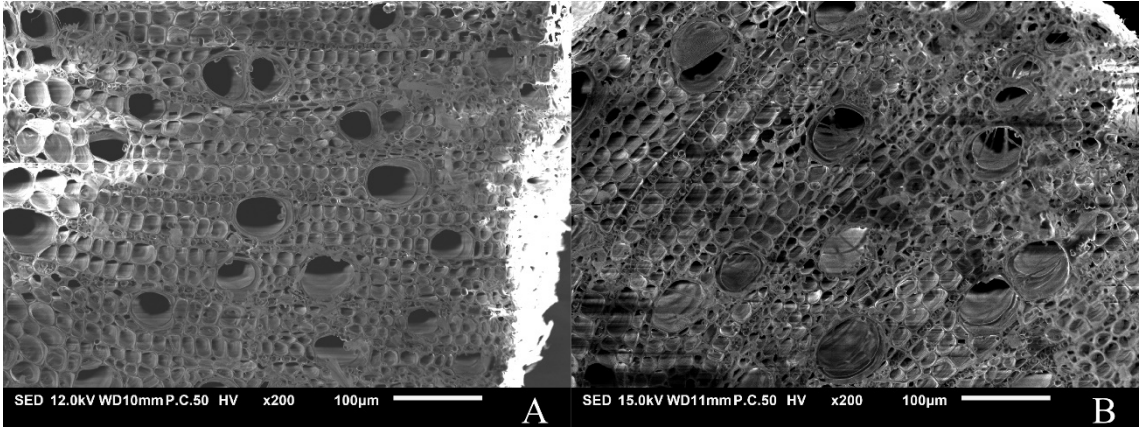
601 Lines correspond to GAB model, Eq. (2).

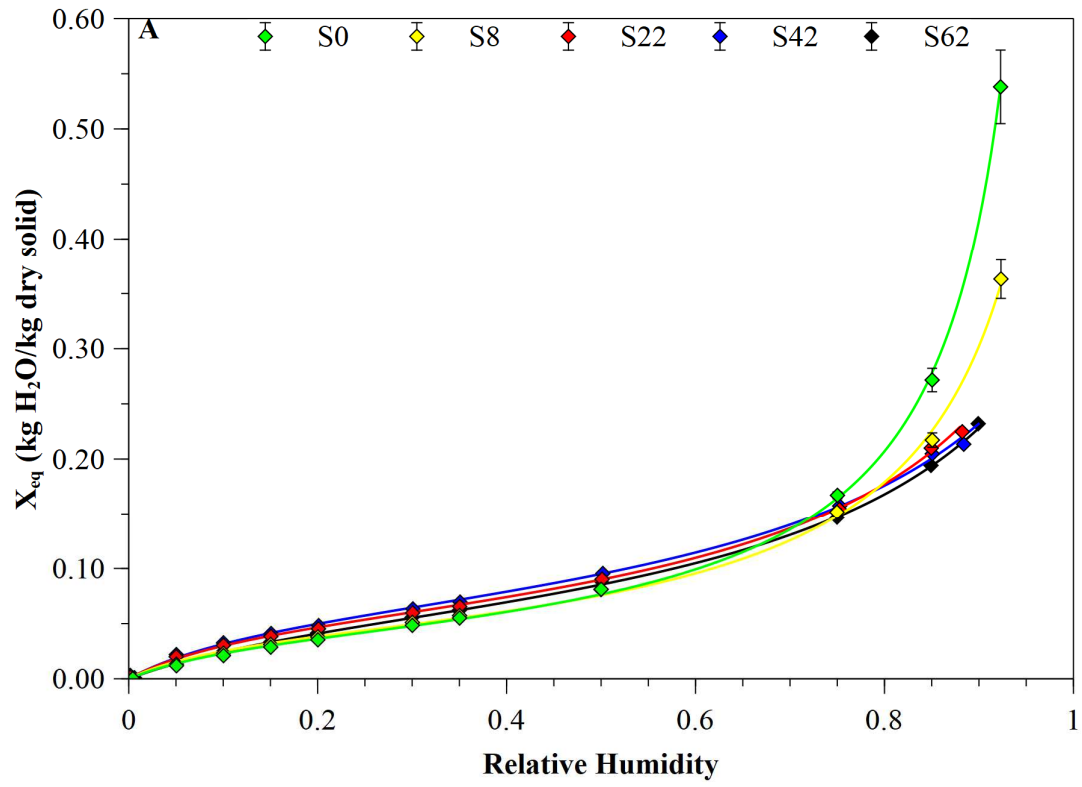
602 **Figure 5a.** Water absorption kinetics (WA_{M0} and WA_{MF}) and solid loss (SL) of hemp shiv
603 retted 22 days. Lines correspond to Nagy and Vas model, Eq. (8).

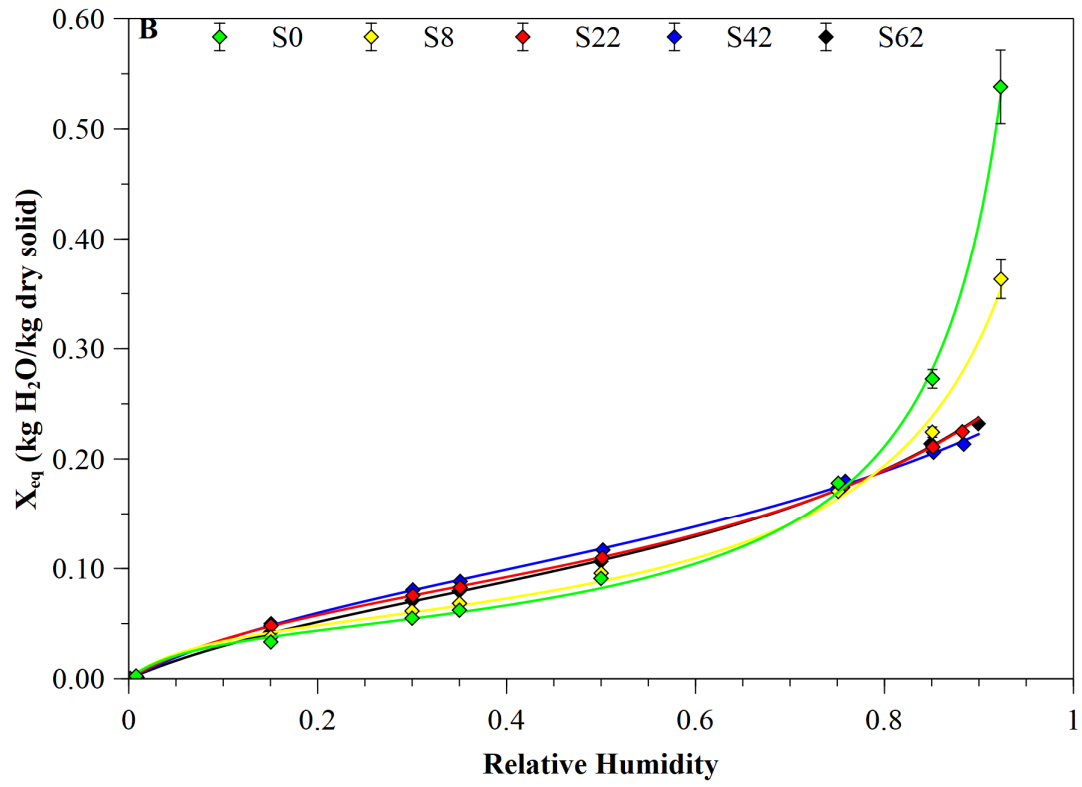
604 **Figure 5b.** Water absorption (WA_{M0}) of hemp shiv retted during different time periods.

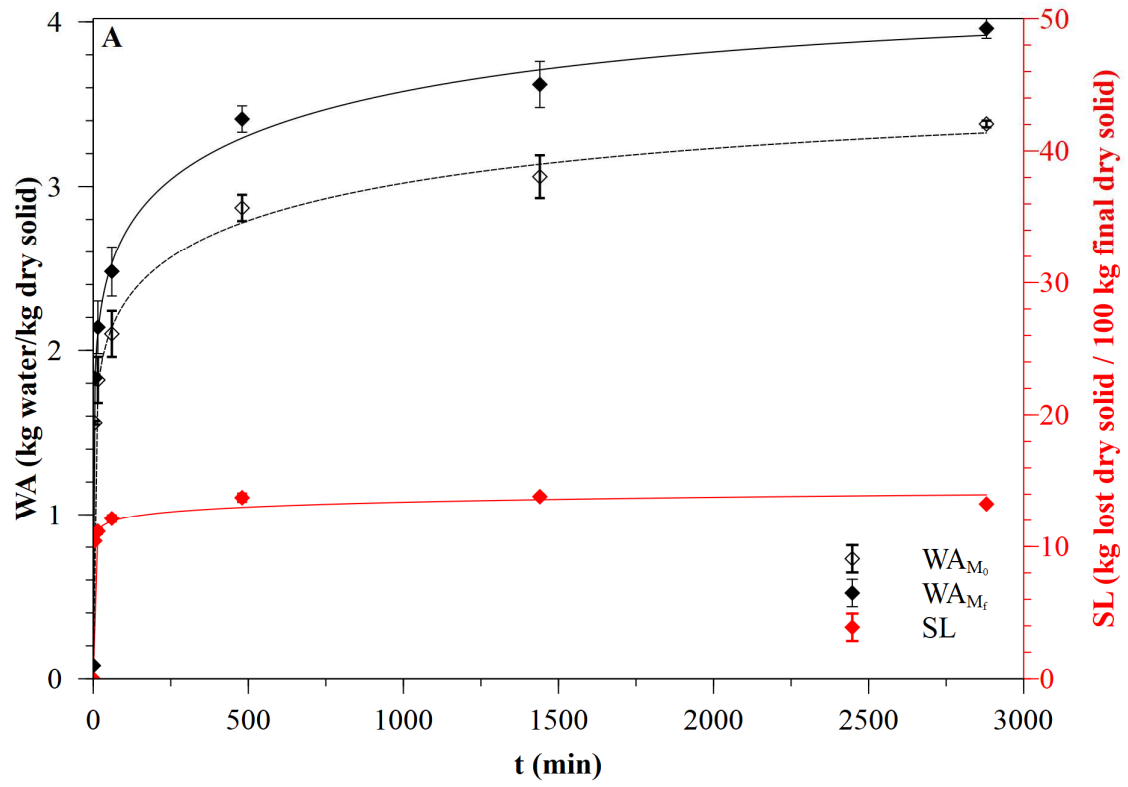












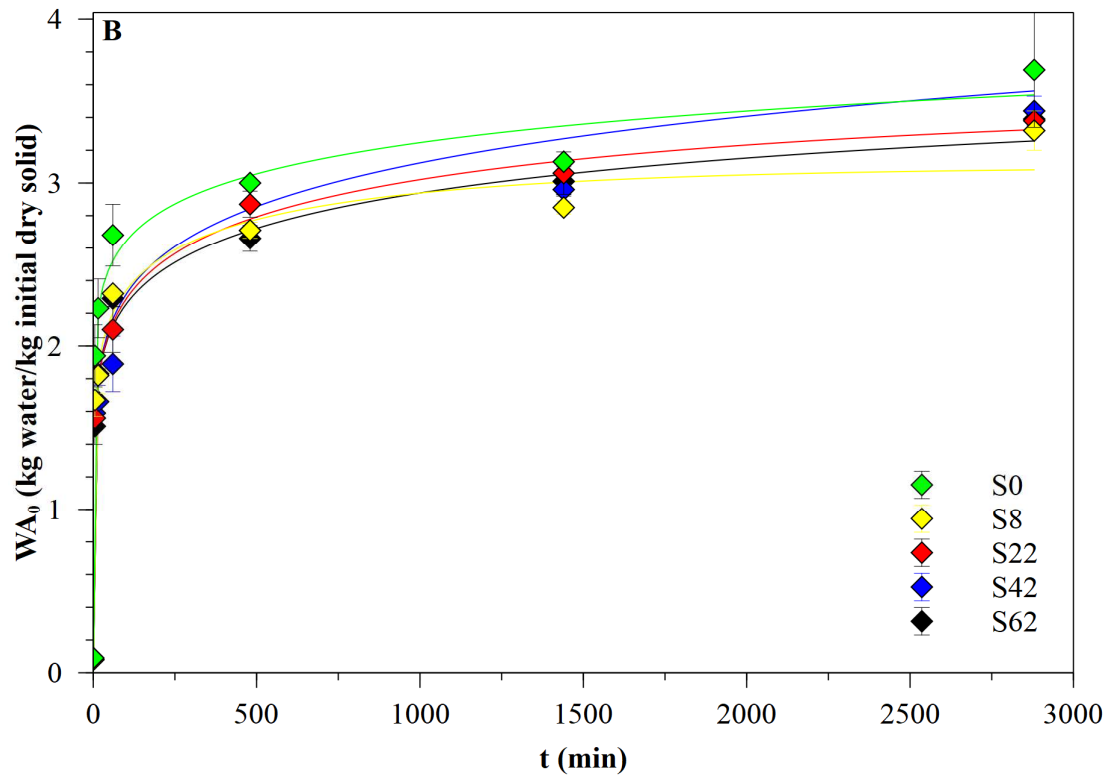


Table 1. True and envelope density, closed porosity (θ_{closed}), chemical composition and colour parameters of hemp shiv retted during different days.

Sample	S0	S8	S22	S42	S62
ρ_{envelope} (kg/m ³)	739±10 ^b	673±7 ^b	700±9 ^b	1159±63 ^a	1139±21 ^a
ρ_{pwall} (kg/m ³)	1463±7 ^b	1479±8 ^b	1491±7 ^b	1555±12 ^a	1553±14 ^a
θ_{closed} (-), Eq. (1)	0.49	0.54	0.53	0.25	0.27
Mass loss (g/ 100 g dry solid)	-	3.1±0.4 ^a	19.6±0.2 ^{a,b}	20.2±0.6 ^b	26.6±4.0 ^b
Soluble (g/ 100 g dry solid)	21.1±0.3 ^c	17.2±0.3 ^b	12.9±0.1 ^a	13.1±0.7 ^a	12.3±0.3 ^a
Hemicellulose (g/ 100 g dry solid)	21.5±0.5 ^a	22.4±1.3 ^a	16.8±1.1 ^b	15.3±1.5 ^{b,c}	11.9±2.1 ^c
Cellulose (g/ 100 g dry solid)	46.1±0.1 ^c	46.3±1.1 ^c	41.3±1.2 ^b	42.6±1.0 ^b	39.4±1.7 ^c
Lignin (g/ 100 g dry solid)	8.5±0.2 ^a	8.9±0.3 ^a	8.6±0.2 ^a	7.6±0.1 ^a	7.5±0.2 ^a
Ash (g/ 100 g dry solid)	2.8±0.1 ^d	2.2±0.2 ^d	1.7±0.1 ^b	1.2±0.1 ^a	1.3±0.1 ^a
L*	84.61±0.63 ^a	84.08±0.43 ^a	82.25±0.73 ^a	71.12±1.08 ^b	64.47±0.38 ^a
a*	-0.62±0.26 ^a	0.38±0.09 ^b	1.11±0.15 ^c	0.50±0.06 ^b	1.22±0.07 ^c
b*	19.78±0.44 ^d	16.14±0.46 ^c	13.61±0.31 ^b	9.55±0.33 ^a	9.57±0.22 ^a

*Data are presented as mean ± standard deviation. Data values in a row with different superscript letters are significantly different at the $p \leq 0.05$ level.

Table 2. GAB (Eq. (2)) and BET (Eq. (3)) parameters and their corresponding statistical coefficients (R^2 , E_{RMS}) values for water sorption isotherms of hemp shiv retted from 0 to 62 days.

Model	Parameters	Adsorption					Desorption				
		S0	S8	S22	S42	S62	S0	S8	S22	S42	S62
	C (-)	8.3±1.2 ^a	10.1±0.2 ^a	9.2±0.2 ^a	8.9±0.1 ^a	6.4±0.1 ^b	15.7±3.5 ^a	14.8±1.3 ^a	8.1±0.2 ^b	6.5±0.2 ^c	5.7±0.3 ^c
	K (-)	0.998±0.004 ^a	0.952±0.005 ^b	0.854±0.002 ^c	0.808±0.001 ^e	0.829±0.003 ^d	0.994±0.006 ^a	0.929±0.010 ^b	0.740±0.001 ^c	0.629±0.005 ^d	0.730±0.015 ^c
GAB	X_m (d.b.)	0.043±0.001 ^d	0.044±0.001 ^d	0.059±0.001 ^c	0.066±0.001 ^a	0.061±0.001 ^b	0.044±0.001 ^d	0.051±0.001 ^c	0.084±0.001 ^b	0.108±0.001 ^a	0.089±0.003 ^b
	R^2 (-)	0.9998	0.9992	0.9997	0.9995	0.9997	0.9993	0.997	0.9999	0.9997	0.9996
	E_{RMS} (d.b.)	0.005	0.006	0.001	0.002	0.002	0.006	0.007	0.001	0.002	0.003
	C (-)	6.1±0.1 ^e	7.1±0.2 ^c	11.0±0.1 ^b	11.6±0.1 ^a	6.7±0.1 ^d	-	-	-	-	-
	X_m (d.b.)	0.047±0.001 ^b	0.047±0.001 ^b	0.050±0.001 ^a	0.052±0.001 ^a	0.052±0.001 ^a	-	-	-	-	-
BET	R^2 (-)	0.9999	0.9998	0.998	0.998	0.9992	-	-	-	-	-
	$E_{RMS}10^3$ (d.b.)	0.197	0.248	0.535	0.642	0.480	-	-	-	-	-
	a_s (m ² /g d.s.)	166.0±2.5 ^c	167.3±2.3 ^c	177.0±1.0 ^b	186.0±1.7 ^a	184.3±2.0 ^a	-	-	-	-	-

*BET model was applied for experimental data between 0.05 and 0.035 of relative humidity. ** d.b. : kg water/kg dry solid. ***Data are presented as mean ± standard deviation. Data values in a row (adsorption and desorption independently) with different superscript letters are significantly different at the $p \leq 0.05$ level.

Table 3. Nagy and Vas model, Eq. (8), parameters for water absorption and solid loss kinetics of hemp shiv retted during different time periods.

Parameters		S0	S8	S22	S42	S62
WA _{M0}	WA _{M0∞} (kg water/ kg dry solid)	4.6	4.0	4.1	3.8	3.9
	A (-)	0.008	0.008	0.008	0.008	0.008
	K (-)	0.097	0.117	0.133	0.150	0.126
	R ² (-)	0.991	0.993	0.997	0.988	0.992
	E _{RMS} (kg water/ kg dry solid)	0.1	0.1	0.1	0.1	0.1
WA _{MF}	WA _{MF∞} (kg water/ kg dry solid)	3.6	3.3	3.4	3.4	3.4
	A (-)	0.008	0.008	0.008	0.008	0.008
	K (-)	0.094	0.110	0.133	0.150	0.127
	R ² (-)	0.986	0.989	0.997	0.986	0.991
	E _{RMS} (kg water/ kg dry solid)	0.1	0.1	0.1	0.1	0.1
SL	SL _∞ (kg lost solid/ kg dry solid)	20.2	15.8	13.6	11.5	10.9
	A (-)	0.289	0.071	0.123	0.014	0.200
	K (-)	0.172	0.110	0.072	0.078	0.060
	R ² (-)	0.970	0.992	0.998	0.970	0.997
	E _{RMS} (kg water/ kg dry solid)	1.2	0.5	0.2	0.6	0.2